ISSN 0869-5911, Petrology, 2011, Vol. 19, No. 3, pp. 217–236. © Pleiades Publishing, Ltd., 2011.
Original Russian Text © S.A. Silantyev, A.A. Novoselov, M.V. Mironenko, 2011, published in Petrologiya, 2011, Vol. 19, No. 3, pp. 227–248.

Hydrothermal Systems in Peridotites at Slow-Spreading Ridges. Modeling Phase Transformations and Material Balance: Role of Gabbroids

S. A. Silantyev, A. A. Novoselov, and M. V. Mironenko

Vernadsky Institute of Geochemistry and Analytical Chemistry, Russian Academy of Sciences, Kosygina 19, 117975 Moscow, Russia
e-mail: silantyev@geokhi.ru

Received September 21, 2010; in final form, October 12, 2010

Abstract—This work was aimed on the estimation of role of gabbro in the ore mobilization during hydrothermal transformation of oceanic (gabbro–peridotite) crust at slow-spreading mid-ocean ridges. Kinetic–thermodynamic modeling was used to reconstruct the geochemical and mineralogical trends of evolution of gabbroids during their hydrothermal interaction with marine fluid. The results of our simulation offered a new insight into some problems of material balance and ore formation during hydrothermal process in the slow-spreading mid-ocean ridges. It was shown that the root zones of all known MAR hydrothermal fields related to serpentinites are made up of ultrabasic rocks and located within peridotite protolith near hot and uncooled gabbroic bodies. It was also demonstrated that the observed mineral and geochemical diversity of metagabbros of slow-spreading mid-ocean ridges was provided by the interaction of hydrothermal fluid percolating through the Hess-type oceanic crust with gabbro bodies. It was established that almost cooled gabbroid bodies, being involved in hydrothermal circulation in the shallow root zones, may play an important role in the redistribution of the material within the Hess-type oceanic crust.

DOI: 10.1134/S0869591111030027

INTRODUCTION

This is the final paper in a series of works (Silantyev et al., 2009a, 2009b) dealing with simulation of geochemical and mineralogical effects that accompany hydrothermal transformation of ultrabasic rocks in the slow-spreading ridges at the downwelling and upwelling limbs of circulation hydrothermal system.

Studies carried out in the axial zone of the Mid-Atlantic Ridge (MAR) for the last two decades (for instance, Cannat et al., 1992; Silantyev, 1998; Fujiwara et al., 2003, *Shipboard...*, 2003) established that gabbroids may occupy about 50 vol % of the oceanic crust of slow-spreading ridges, are closely associated with serpentinites, and widely developed in the mantle protolith of the oceanic lithosphere below Moho discontinuity. Since gabbroids compose the "oceanic core complexes" hosting all largest hydrothermal ore fields of Central Atlantics (Ashadze, Semenov, Logachev, and Rainbow fields), they are involved into ore-forming hydrothermal processes.

The main aim of this work was to estimate the role of gabbro in mobilization of ore material during hydrothermal alteration of the oceanic crust section consisting of gabbro–peridotite associations (Hess-type crust) in slow-spreading mid-ocean ridges (MOR). The geochemical and mineralogical trends of gabbroid evolution during their hydrothermal interaction with marine fluid were reconstructed using kinetic–thermodynamic simulation, which, as in the recently published works (Silantyev et al., 2009a, 2009b) represented the main tool of our study.

A great body of presently accumulated data on geochemistry and mineralogy of gabbroids of slow-spreading MOR indicates an unambiguous involvement of these rocks in the hydrothermal transformation of the Hess-type oceanic crust. As was noted in (Silantyev et al., 1987), conditions existing in MOR were favorable for the formation of vertical metamorphic zoning in the zones of active hydrothermal systems. From the top downward, this zoning is represented by metabasic rocks metamorphosed under the zeolite (≤300°C), greenschist (300–500°C), and epidote–amphibolite (500–650°C) facies conditions. Numerous later works demonstrated that practically all samples of gabbroids from the oceanic core complexes of MAR contain secondary mineral assemblages that were formed within a wide temperature range varying from the lower greenschist to the upper amphibolite facies (for instance, Gillis et al., 1993; Silantyev, 1998; Fletcher et al., 1997). The characteristic feature of secondary aluminous hornblende in MAR gabbroids is the high Cl content (up to 1.2–2.0 wt %) in the anionic group (Vanko, 1986; Silantyev et al., 1987). Taking into account extremely low chlorine content in the magmatic derivatives of MAR (for instance, Jambon, 1994), the source of chlorine in the metamorphic system responsible for the formation of high-Cl hornblende in the

MAR gabbroids was presumably mineralized marine fluid. Data on the presence of high-salinity fluid inclusions in secondary amphibole, epidote, quartz, and plagioclase (Stakes and Vanko, 1986; Kelley and Delaney, 1987; Simonov et al., 1987; Simonov et al., 1995) also can serve as a convincing argument for the participation of such fluid in high-temperature hydrothermal transformation of oceanic gabbroids. Using experimental results, Mottl (1983) revealed that Fe mole number of amphibole and coexisting chlorite from metabasic rocks of oceanic hydrothermal systems systematically increases with decreasing W/R (water/rock) ratio. In (Silantyev et al., 1987), this trend was explained by the compositional evolution of hydrothermal fluid, whose interaction with host rocks in the upper crustal horizons (high W/R ratio) leads to the extraction of iron and its transfer to the deeper seated crustal levels, with formation of Fe-rich amphibole and chlorite.

Recently obtained data on the behavior of stable and radiogenic isotope systems in the gabbroids and serpentinites from the oceanic core complexes of MAR demonstrated a complex evolution of isotope composition of marine fluid interacting with these rocks in a wide temperature regime: for sulfur (Alt et al., 2007; Delacour et al., 2008), for oxygen (Alt et al., 2007), for strontium (Silantyev and Kostitsyn, 1990). Oxygen and sulfur isotope data on gabbroids recovered by boreholes ODP 1268 and 1271 in the MAR axis immediately north of the Logachev field indicate high-temperature (>350°C) interaction of these rocks with hydrothermal fluid at deep levels of crustal section (Alt et al., 2007). In (Silantyev and Kostitsyn, 1990), the Sr content and isotope compositions in secondary minerals from oceanic metagabbro were used to reconstruct the exhumation of the metagabbroids from the oceanic core complex located in the junction zone of MAR and 15°20′ Fracture Zone. Results obtained in this work clearly demonstrated a systematic increase of $^{87}Sr/^{86}Sr$ in a series of secondary minerals with decreasing temperature of their formation: 0.7044 in *Hbl* (550°C), 0.7060 in Al-*Act* (450°C), 0.7070 in *Act* (300°C), 0.7080 in *Sap* + *Chl* (150–200°C)[1].

The role of gabbro in the hydrothermal process in the axial zone of MAR was discussed in (Sharkov et al., 2007). These authors arrived at conclusion that gabbroid intrusions formed during evolution of water-saturated melts that produced siliceous Fe–Ti oxide series (terminology of E.V. Sharkov with co-authors) could be sources for the ore-bearing fluids. According to (Sharkov et al., 2007), among gabbroids of this type are hornblende gabbros of MAR.

The works devoted to the simulation of geochemical and mineralogical variation trends of gabbroids during their hydrothermal interaction with marine fluid are few in number. Thermodynamic model of hydrothermal alteration of the lower part of the oceanic crust consisting of gabbro was proposed in the work (McCollom and Schock, 1998). In this work, the interaction of marine fluid with olivine gabbros, gabbronorites, and troctolites at temperature 300–900°C were simulated by mathematical methods. An important achievement of model proposed in (McCollom and Shock, 1998) was theoretical confirmation of high-temperature (≥700°C) interaction of marine fluid with deep-seated oceanic rocks, which was discovered empirically in (Kelley and Delaney, 1987; Silantyev, 1998).

The only attempt to thermodynamically simulate the downwelling limb of hydrothermal system in the MOR section containing gabbro–peridotite association was made in (Silantyev et al., 1992). One of the principle conclusions obtained form this work was the existence of geochemical barriers at the peridotite–gabbro boundary, where secondary accumulation and precipitation of ore material are possible.

Thus, the gabbroid bodies as ubiquitous components of geological section of the oceanic crust of the slow-spreading MAR may not only serve as thermal source for hydrothermal circulation system (Silantyev et al., 2009a), but also control the material balance in the hydrothermal process.

SIMULATION TECHNIQUE

In the previous works (Silantyev et al., 2009a, 2009b), we proposed a generalized model of hydrothermal system located in the Hess crust section made up of mantle peridotites (spinel harzburgites). All peridotite section was subdivided into 22 blocks with certain T and P parameters, through which fluid portions (10 waves) were successively passed. Interactions between fluids and minerals in the rock were analyzed for each block with allowance for kinetics of their dissolution. In order to simulate the interaction at the upwelling limb, we used compositions of fluid that enters the root zone at the second wave, because the downwelling system reaches stationary regime during this wave.

In this work, the model crustal section considered in the previous works (Silantyev et al., 2009a, 2009b) was supplemented by block of gabbroids, which was placed in the root zone of hydrothermal system and interacted with hydrothermal fluid of given composi-

[1] Mineral abbreviations accepted in the work: (*Act*) actinolite, (*Amph*) amphibole, (*Anh*) anhydrite, (*Arg*) aragonite, (*Ant*) antigorite, (*Bn*) bornite, (*Brc*) brucite, (*Ccp*) chalcopyrite, (*Cc*) chalcosine, (*Chl*)—chlorite, (*Ctl*) chrysotile, (*Cv*) covellite, (*Cz*) clinozoiste, (*Di*) diopside, (*Dol*) dolomite, (*Fa*) fayalite, (Fe-*Act*) Fe-actinolite, (Fe-*Prg*) Fe-pargasite, (*Fo*) forsterite, (*Gn*) galena, (*Gt*) goethite, (*Hbl*) hornblende, (*Hd*) hedenbergite, (*Hem*) hematite, (*Mag*) magnesite, (Mg-*Sap*) Mg-*saponite*, (*Mt*) magnetite, (Na-@Sap) Na-saponite, (*Ol*) olivine, (*Prh*) prehnite, (*Py*) pyrite, (*Po*) pyrrhotite, (*Qtz*) quartz, (*Sap*) saponite, (*Sp*) sphalerite, (*Spl*) spinel, (*Srp*) serpentine, (*Tlc*) talc, (*Tr*) tremolite, (*Zo*) zoisite).

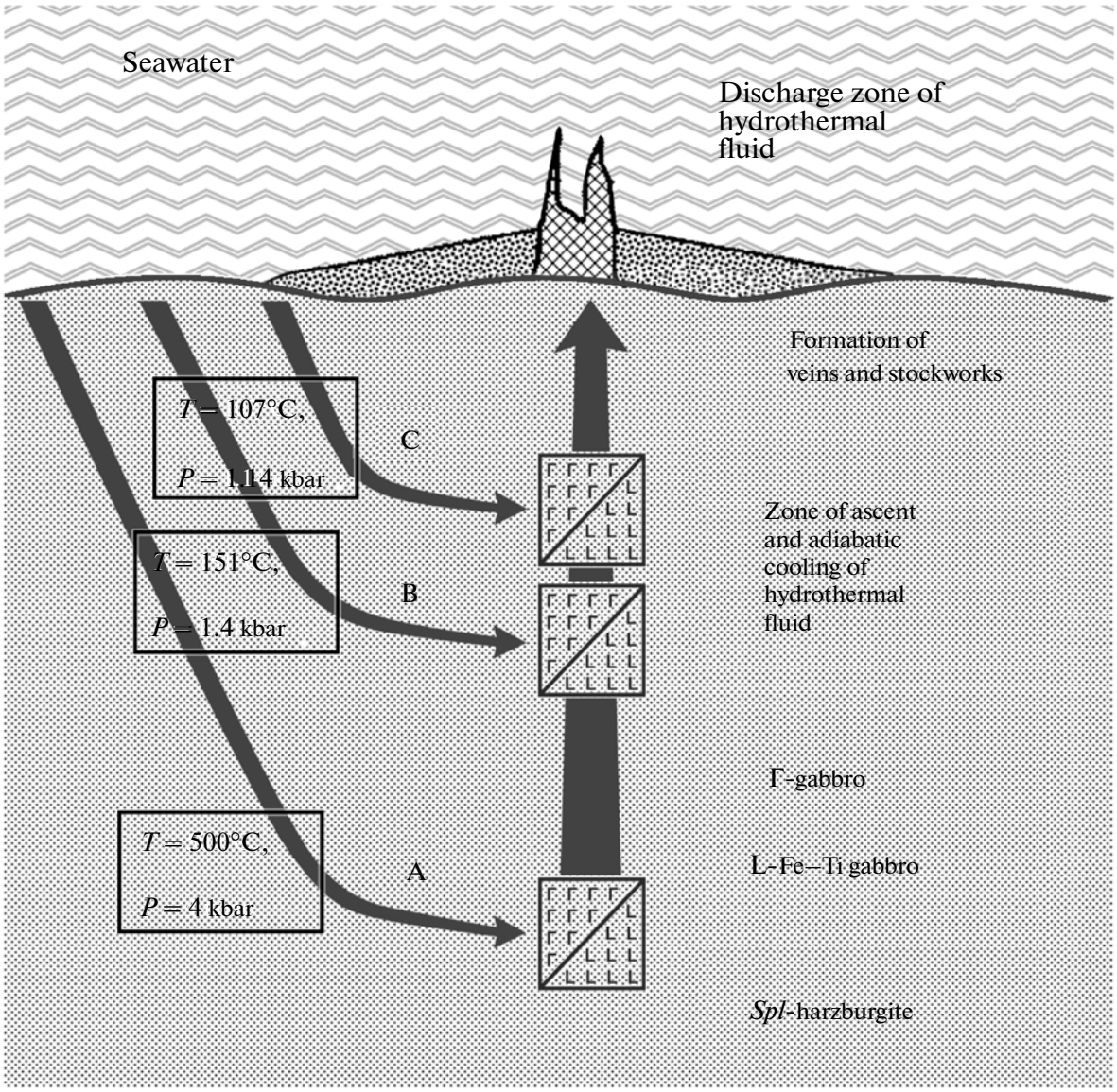

Fig. 1. Schematic representation of the gabbroid root zone of hydrothermal system of the Hess-type crust. (A) high-temperature root zone (located at a section depth about 11 km); (B) moderate–low temperature root zone (section depth of 3 km); (C) low-temperature root zone (section depth of 2 km). Cross hatching denotes hydrothermal edifices, speckled areas correspond to hydrothermal precipitates.

tion. As in (Silantyev et al., 2009b), three possible variants of the location of the root zone of hydrothermal circulation system were analyzed: (1) significant depths $T = 500°C$, $P = 4$ kbar, (2) moderate–shallow depths $T = 151°C$, $P = 1.4$ kbar, and (3) shallow depths $T = 107°C$, $P = 1.14$ kbar (A, B, C in Fig. 1). Hydrothermal fluids interacting with the gabbroid blocks in composition corresponded to the fluids that percolated through peridotite column to three depth levels of the indicated root zones. The compositions of fluids that entered these root zones were taken from (Silantyev et al., 2009a) and are shown in Table 1. Calculations used two contrasting gabbroid compositions that embrace the most part of compositional range of oceanic gabbro: ophitic (normal) gabbro and Fe–Ti gabbros. According to the classification proposed by (Miyashiro and Shido, 1980), one of these compositions corresponds to the gabbro of the middle stage of the evolution of MAR plutonic complex, whereas other marks the late-stage gabbroids enriched in ore elements. Normal gabbro (sample SeDV4-9) is represented by coarse-grained rock with well-pronounced ophitic texture and consisting of plagioclase, clinopyroxene, orthopyroxene, and secondary amphibole. Other sample used in our work (sample SeDV4-2) is gabbro enriched in ore minerals, whose aggregates define sideronite texture of the rock. This sample is made up plagioclase, ortho- and clinopyroxene, abun-

Table 1. Composition of solutions that supplied in the root reaction zones, mol/kg of H_2O

Components	$T = 107°C$, $P = 1140$ bar	$T = 151°C$, $P = 1460$ bar	$T = 500°C$, $P = 4000$ bar
ΣCO_2	3.815E-05	9.058E-19	6.557E-18
CH_4	3.852E-24	2.691E-05	5.212E-05
H_2	6.087E-12	4.895E-02	2.236E+00
ΣH_2S	3.699E-16	6.783E-04	8.494E-03
Mg	4.175E-02	1.522E-07	6.856E-04
Ca	1.456E-02	7.745E-02	4.413E-02
Al	1.622E-07	2.253E-04	1.119E-05
Si	1.107E-07	5.980E-05	1.624E-02
Na	4.885E-01	5.110E-01	9.857E-01
ΣSO_4	1.296E-02	8.336E-24	5.920E-20
Cl	5.606E-01	5.871E-01	1.080E+00
Fe	7.881E-08	1.314E-04	1.899E-03
Cu	1.094E-05	2.899E-09	1.526E-04
Zn	6.107E-05	2.564E-08	5.248E-04
Pb	1.187E-07	1.279E-10	7.862E-06
pH	7.639	9.898	5.053

Table 2. Alteration of gabbro and Fe–Ti gabbro from reaction zones during interaction with hydrothermal fluids, wt % (100%—starting rock)

Components	Unaltered rock		$T = 107°C$, $P = 1140$ bar		$T = 151°C$, $P = 1460$ bar		$T = 500°C$, $P = 4000$ bar	
	gabbro	Fe-Ti gabbro	gabbro	Fe-Ti gabbro	gabbro	Fe-Ti gabbro	gabbro	Fe-Ti gabbro
MgO	8.81	7.33	9.0000	7.5108	8.5503	6.9591	7.4639	5.3114
CaO	9.32	9.61	9.1085	9.4138	9.4784	9.6802	4.6347	7.2180
Al_2O_3	13.49	12.59	13.4978	12.5901	13.0644	12.0276	9.2002	11.7754
SiO_2	49.82	38.16	49.8406	38.1670	48.3393	36.0666	39.5383	31.9536
TiO_2	3.01	6.43	3.0094	6.4282	3.0094	6.4282	3.0094	6.4282
Na_2O	2.88	2.01	2.8559	1.9760	2.4831	1.4217	2.9405	1.9668
FeO*	12.66	23.84	12.6643	23.8699	12.2978	22.8575	12.2685	22.7449
Cu	0.0174	0.0161	0.0158	0.0044	0.010817	0.006368	0.000135	0.000027
Zn	0.0057	0.0123	0.0064	0.0077	0.005498	0.008539	0.000044	0.000069
Pb	0.0012	0.0021	0.0013	0.0021	0.000236	0.000401	0.000010	0.000004

dant Ti-magnetite, ilmenite and secondary amphibole. Both the samples were taken in the Ashadze hydrothermal field (Shipboard..., 2007), and their compositions are shown in Table 2. On the basis of petrographic and geochemical characteristics, the rocks used for simulation can be ascribed to the typical representatives of gabbroids of the MAR oceanic core complexes.

A sequence of chemical transformations of the fluid in the course of its filtration and variations in the P–T parameters were simulated as a series of partial isobaric–isothermal equilirbia, while masses of interacting primary minerals were limited by the rates of their dissolution. It was accepted that hydrothermal fluid does not have enough time to react with the host rocks and primary minerals during its transportation from the root zone to the discharge zone. Thus, at the upwelling limb of hydrothermal system we considered only the processes of precipitation and gas release. In order to calculate the adiabatic drop in fluid temperature in the discharge zone, we applied the International System of Equations 1995 (IAPWS-95) for the thermodynamic properties of water and aqueous vapor, which was proposed for calculations in industrial processes (Wagner and Pruss, 2002). As in the previous works (Silantyev et al., 2009a, 2009b), the calculations were carried out using a GEOCHEQ software package (Mironenko et al., 2000). The system

involved 15 components: O–H–Si–Ti–Al–Mg–Fe–Ca–Na–Cl–S–C–Zn–Pb–Cu. The gas phase consisted of 7 components: CH_4, CO, H_2, H_2O, CO_2, O_2, and H_2S. The fugacity coefficients of gases and compressibility of gas mixture were calculated using the Peng-Robinson equation. Principle ore phases in the model system were pyrrhotite, sphalerite, chalcopyrite, chalcosine, bornite, galena, pyrite, covellite, and native copper. The following complexes of ore elements were considered in the solution: $CuCl^0$, $Cu(HS)_2^-$, $Cu(OH)_2^-$, Cu^+, $CuCl^+$, Cu^{+2}, $CuCl_2^-$, $CuCl_2^0$, $CuCl_3^-$, $CuCl_4^{-2}$, $CuHS^0$, CuO^0, CuO_2^{-2}, $CuOH^0$, $CuOH^+$, $HCuO_2$, $HZnO_2^-$, $ZnOH^+$, Zn^{+2}, $ZnCl^+$, $ZnCl_2^0$, $ZnCl_3^-$, ZnO^0, ZnO_2^{-2}, $HPbO_2^-$, $PbCl_4^{-2}$, $Pb(HS)_2^0$, $Pb(HS)_3^-$, Pb^{+2}, $PbCl^+$, $PbCl_2^0$, $PbCl_3^-$, PbO^0, $PbOH^+$, $FeCl^+$, Fe^{+3}, Fe^{+2}, $FeCl^{+2}$, $FeCl_2^0$, FeO^0, FeO^+, FeO_2^-, $FeOH^+$, $FeOH^{+2}$, $HFeO_2^-$, $HFeO_2^0$.. The complexes were treated with the use of parameters in the HKF-model taken from (Shock et al., 1997; Sverjensky et al., 1997). These parameters were made consistent with the data base in (Johnson et al., 1992), which serves as the basis for thermodynamic information in GEOCHEQ.

Kinetic–thermodynamic simulation of mineral formation in the root zones of hydrothermal systems consisting of the gabbro–peridotite association was made by the similar manner as in (Silantyev et al., 2009a), and was limited by kinetics of mineral dissolution (Zolotov and Mironenko, 2007).

RESULTS OF SIMULATION OF PHASE TRANSFORMATIONS AND MATERIAL BALANCE DURING INTERACTION OF HYDROTHERMAL FLUID WITH GABBRO

Root Zone

Phase transformations in gabbroids. Figure 2 demonstrates a scheme of mineral transformations obtained for two considered petrographic types of gabbroids during their interaction with second wave of hydrothermal fluid that percolated through peridotite section up to depths of reaction (root) zones corresponding to 107°C, 151°C, and 500°C (C, B, and A in Fig. 1). The gabbro–fluid interaction in the root zone is accompanied by the formation of phase assemblages shown in Fig. 2. Taking into account the duration of percolation of hydrothermal fluid to the root zones considered in our modeling (Silantyev et al., 2009a), the time of formation of the indicated mineral assemblages in the gabbroid block after the onset of hydrothermal circulation was estimated to be within the following ranges: 4270–4950 years (low-temperature root zone C), 5420–5960 (moderate–low-temperature root zone B), and 7946–7951 years (high-temperature root zone A).

Normal (ophitic) gabbro

Root zone of 107°C. Judging from calculations, pyrite was first to dissolve among primary minerals of the ophitic gabbro. Its disappearance is accompanied by the monotonous decrease of fluid pH (from 7.4 to 6), which, however, again increases to 7 during further fluid interaction with gabbro. Olivine and clinopyroxene start to dissolve only during longer term interaction of fluid with ophitic gabbro. In general, primary silicate phases of ophitic gabbro during its low-temperature interaction with fluid show significantly higher stability than those of spinel harzburgites.

The first products of hydrothermal transformations of ophitic gabbro are represented by the brucite + hematite + zeolite + chrysotile + clinochlore + daphnite + tremolite assemblage. Such a mineral assemblage is formed during decrease of fluid pH from 7.4 to 6. Among early accessory ore phases are galena, chalcosine, zincite (ZnO), native copper, and sphalerite (during longer term interaction). It should be noted that these minerals occupy an insignificant volume of hydrothermally altered ophitic gabbro (from 10^{-2} to 10^{-6} vol %). The rock also contains negligible ($<10^{-6}$ vol %) amounts of titanite. The longer term interaction (about 100 years after the influx of the second wave of fluid in the gabbroic reactor or about 6000 years after the onset of fluid transportation along downwelling limb) in the ophitic gabbros leads to the formation of assemblage chlorite + prehnite + zeolite (stilbite) + epidote + tremolite + chrysotile. Minerals that compose this assemblage account significant part of volume of hydrothermally altered gabbro (Fig. 2a). Therefore, this assemblage could be considered as indicator assemblage for the metagabbro from the low-temperature root zone of hydrothermal system located in the serpentinite protolith.

Root zone of 151°C. In general, the sequence of dissolution of primary minerals in the ophitic gabbro from moderate–low-temperature root zone is similar to that established for the low-temperature zone. However, at temperature of 151°C, olivine and clinopyroxene are dissolved more rapidly. Orthopyroxene and, to a lesser extent, plagioclase, remain practically unchanged at this temperature.

At the initial stages of hydrothermal transformation of the gabbroids (at temperature of 151°C), fluid pH decreases from 9.9 to 7.3. This is accompanied by the formation of chlorite + prehnite + clinozoisite assemblage. The longer term interaction with fluid (100 years after the influx of second fluid wave into reactor and about 5400 years after onset of fluid transport along downwelling limb) provides the formation of lomontite + stilbite + stellerite assemblage. Accessory minerals of this assemblage are represented by

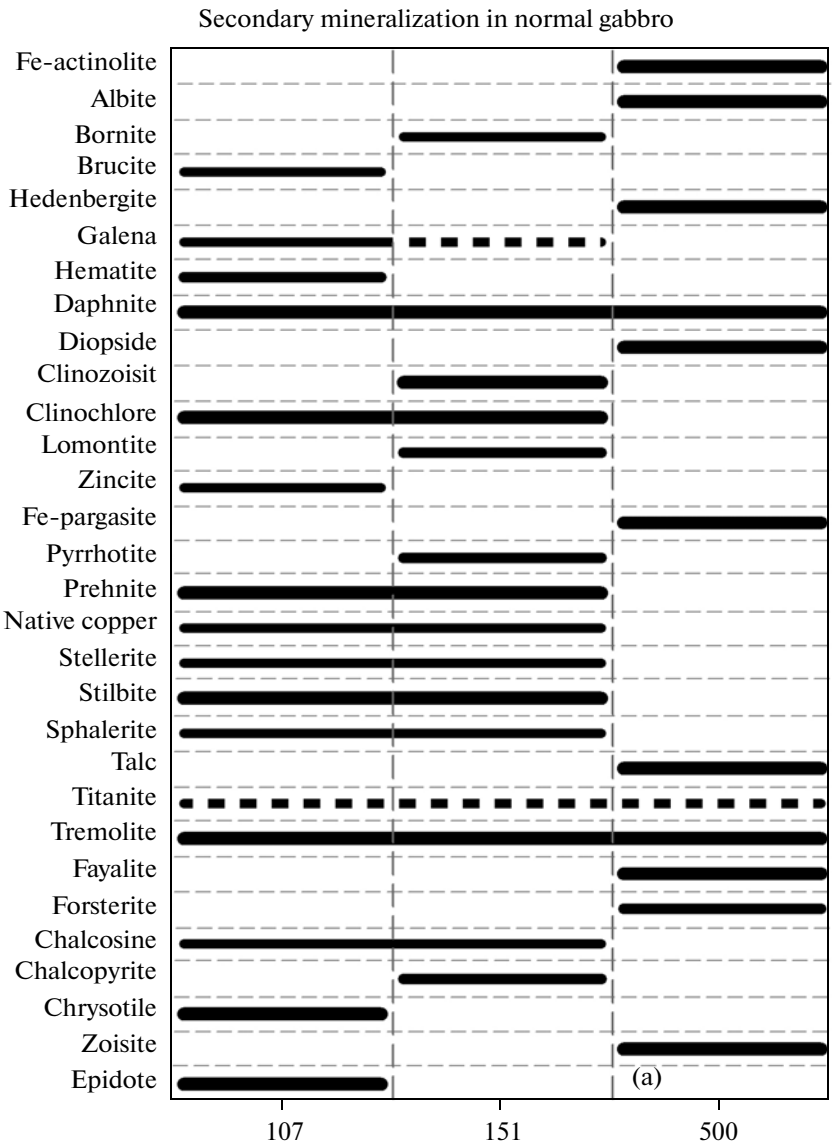

Fig. 2. Mineral composition of the root zone gabbroid of hydrothermal systems after their interaction with hydrothermal fluid. Solid line denotes the volume of mineral phase $>10^{-2}$ vol %, thin line show 10^{-2} to 10^{-6} vol %, dashed line $<10^{-6}$ vol %; (a) ophitic gabbro, (b) Fe–Ti gabbro.

native copper and sphalerite, which are later supplemented by pyrrhotite, chalcosine, chalcopyrite, and bornite. The rock also contains negligible ($<10^{-6}$ vol %) amounts of titanite and galena. The indicator mineral assemblage of metagabbro from the low-temperature root zone is represented by chlorite, clinozoisite, prehnite, stilbite, and tremolite and was formed after 100 years of onset of fluid–rock interaction at temperature of 151°C (Fig. 2a). Thermodynamic calculations demonstrated an increase in stellerite content in the newly formed zeolites of the moderate–low temperature hydrothermal system as compared to the low-temperature system. Fridriksson et al. (2001) studied compositional variations of zeolite (in a series stilbite ($Ca_2NaAl_5Si_{13}O_{36} \cdot 16H_2O$)–stellerite ($Ca_2Al_4Si_{14}O_{36} \cdot 14H_2O$) in the metabasic rocks with increasing temperature and depth. Data presented in this work indicate a systematic increase of stellerite in the stilbite–stellerite solid solution with increasing depth and section temperature. Subsequent growth of temperature leads to the replacement of stilbite by lomontite. Obtained data well reproduce this sequence of mineral formation in the framework of the zeolite facies metamorphism of basic rocks. It should be noted that, both for ophitic and Fe–Ti gabbro (see below), our simulations demonstrated the formation of epidote (in association with prehnite in ophitic gabbro) in the low-temperature root zone, clinozoisite, in the low-temperature zone, and zoisite, in the high temperature zone. A prehnite–epidote equilibrium was studied experimentally in the known work (Liou et

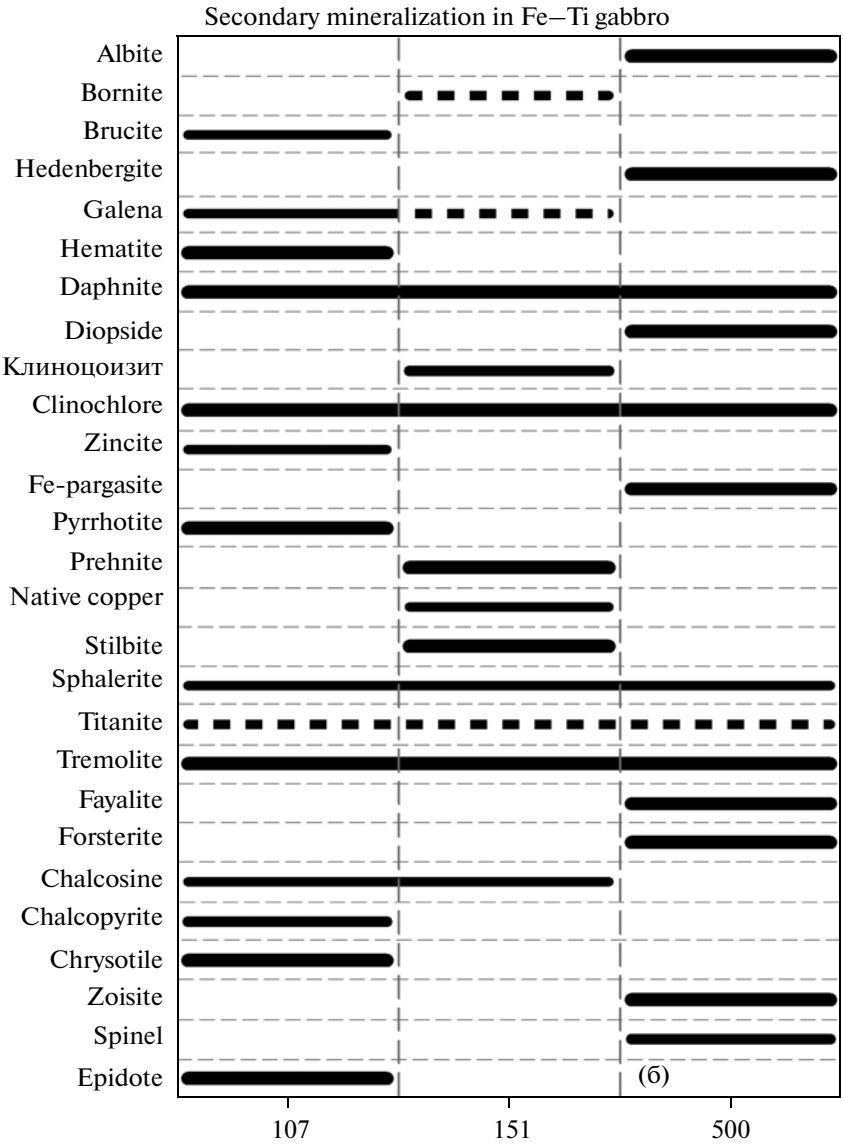

Fig. 2. Contd.

al., 1983). Experimental results showed that epidote and prehnite synthesized under HM-buffer redox conditions and low temperatures have high Fe contents. Under reducing high-temperature conditions, both these phases are depleted in Fe and enriched in Al. Thus, a simulated change of mineral types of epidote in the epidote–zoisite series is well consistent with existing experimental data.

Root zone of 500°C. The high-temperature root zone shows a rapid mineral transformation of the ophitic gabbro in the course of its interaction with hydrothermal fluid. Primary phases in the gabbro from this zone are dissolved more rapidly than in the lower temperature zones and in the following sequence: *Ol* > *Cpx* > *Po* > *Pl*; fluid pH during this process insignificantly decreases. A steady indicator assemblage of secondary minerals in the gabbro from high-temperature root zone appears already at the final stages of operation of hydrothermal reactor and consists of albite, Fe chlorite, Fe-pargasite, talc, zoisite, tremolite, clinopyroxene, olivine (fayalite), Fe-actinolite (more than 0.01 vol %), and sharply subordinate titanite ($<10^{-6}$ vol %) (Fig. 2a). Noteworthy is the complete absence of ore minerals in the secondary mineral assemblage of high-temperature root zone.

Fe–Ti gabbro

Root zone of 107°C. A scheme of dissolution of primary minerals in the Fe–Ti gabbro from the low-temperature root zone is similar to that in the ophitic gabbro. The initial stages of transformation of Fe–Ti gab-

bro lead to the formation of chrysotile + hematite + brucite + zincite (ZnO) + sphalerite + chalcosine assemblage. The longer term interaction with fluid produces a steady chlorite + epidote + hematite + pyrite + tremolite + chrysotile assemblage (more than 0.01 vol %) (Fig. 2b). The rock also contains chalcopyrite, galena, chalcosine, sphalerite ($<10^{-1}$ to 10^{-6} vol %) and subordinate titanite ($<10^{-6}$ vol %). As for the ophitic gabbro, fluid pH here subsequently decreases (from 7.4 to 6) and increases to 8.

Root zone of 151°C. As in the ophitic gabbro, the dissolution of primary olivine and clinopyroxene in the Fe–Ti gabbro at 151°C proceeds efficiently after 100 years of the gabbro–fluid interaction. Data obtained by simulation testify that the indicator assemblage of secondary minerals from the Fe–Ti gabbro of the low-temperature root zone includes chlorite, prehnite, zeolite (stilbite), and tremolite (up to 0.01 vol %); clinozoisite, chalcosine, sphalerite, and native copper occur in lower amounts ($<10^{-2}$ to 10^{-6} vol %) (Fig. 2b). Bornite, galena, and titanite are observed in negligible amounts. The evolution of fluid pH with increasing time of its interaction with rock, as well as in all considered above cases, is characterized by pronounced minimum and subsequent increase (9.9–7.9–9.3).

Root zone of 500°C. The sequence of dissolution of primary phases in the Fe–Ti gabbro from this root zone is similar to that of the ophitic gabbro. As in the ophitic gabbro, efficient transformations of mineral composition of Fe–Ti gabbro in the high-temperature root zone begins practically immediately after influx of fluid in hydrothermal reactor. With change of mineral composition of Fe–Ti gabbro, fluid pH varies from 5.5 to 4.7. Judging from calculation results, a steady indicator assemblage of secondary minerals [albite + chlorite + Fe-pargasite + zoisite + tremolite + clinopyroxene + olivine (> 0.01 vol %)] is formed already during onset of high-temperature hydrothermal transformation of Fe–Ti gabbro. The rock contains also subordinate amounts of sphalerite and secondary spinel ($<10^{-2}$ to 10^{-6} vol %), as well as titanite ($<10^{-6}$ vol %) (Fig. 2b).

Chemical variations in composition of gabbro. Results of simulation showed that the major-element composition of both the considered petrographic types of gabbro, regardless of their starting composition, experience the strongest alterations during their interaction with hydrothermal fluid in the deepest root zone (500°C). These changes consist in the removal of calcium, alumina, silica, magnesium, and iron from the starting rocks (Table 2), at insignificant influx of sodium in the ophitic gabbro and its weak removal from Fe–Ti gabbro. The content of ore elements in the ophitic gabbro remained practically unchanged in the low-temperature and moderate–low-temperature root zones, however, hydrothermal transformation of this rock in the high-temperature zone is accompanied by intense removal of Cu, Zn, and Pb. By contrast, Fe–Ti gabbro demonstrates the loss of ore elements also in the moderate–low-temperature root zone, with the highest removal of Cu, Zn, and Pb in the high-temperature root zone, as in the ophitic gabbro (Table 2).

Variations in composition of hydrothermal fluid

In all above considered scenarios of gabbro interaction with hydrothermal fluid, the latter shows a decrease in pH at the initial stages of gabbro transformation and then increases up to values insignificantly lower than in the starting fluid that entered reactor (Table 3). This effect reflects the dependence of acid–basic properties of fluid on composition of protolith, with which it interacts: starting fluid at given temperature is in equilibrium with ultrabasic rock (harzburgite) and interacts with basic rock (gabbro). Thus, as compared to purely peridotite section, the presence of gabbro in the root zone causes an downward shift of boundary between zones of sharply oxidizing (fluid-predominant) and moderately oxidizing regime for downwelling limb of serpentinite-related hydrothermal systems, which was inferred in (Silantyev et al., 2009a).

In the low-temperature root zone, the concentrations of dissolved gases in fluid for both the types of the considered gabbros at the output of hydrothermal reactor are arranged in the following order: $CO_2 > H_2 > H_2S > CH_4$. Significantly different pattern is observed in the hydrothermal fluid after its interaction with ophitic and Fe–Ti gabbro in the moderate–low-temperature (151°C) and high-temperature (500°C) root zones. The concentrations of dissolved gases in the fluid from these root zones are arranged in the following order: $H_2 > H_2S > CH_4 > CO_2$. Evolution of cationic composition of hydrothermal fluid over the entire range of the considered conditions well correlates with the sequence of mineral formation (Table 3, Fig. 2). Noteworthy is the sharp enrichment of hydrothermal fluid in ore components in the high-temperature root zone.

The results of numerical modeling presented in Table 3 allow us to evaluate the compositional variations of starting hydrothermal fluid that supplied in the root zone, as well as to compare the composition of modified fluid formed during transformation of gabbro with that of fluid from the peridotite root zones, whose compositions are listed in (Silantyev et al., 2009a).

Fluid modified in the low-temperature root zone after interaction with both petrographic types of gabbro at practically unaltered pH shows enrichment in CH_4, H_2S, H_2, as well as Al and Si. The content of all ore elements in it decreases relative to the starting fluid that entered reactor. The hydrothermal fluid from moderate–low-temperature root zone for both gabbro types retains pH of starting fluid, but becomes enriched in Al and Si and depleted in Mg, Ca, and Fe.

Table 3. Variations in the chemical composition of hydrothermal fluid during interaction with gabbro, mol/kg of H_2O

Components	$T = 107°C$, $P = 1140$ bar		$T = 151°C$, $P = 1460$ bar		$T = 500°C$, $P = 4000$ bar	
	gabbro	Fe-Ti gabbro	gabbro	Fe-Ti gabbro	gabbro	Fe-Ti gabbro
ΣCO_2	1.631E-05	1.058E-05	4.185E-19	3.023E-18	4.204E-12	4.118E-12
CH_4	7.335E-18	9.940E-14	2.767E-05	2.811E-05	5.319E-05	5.362E-05
H_2	6.030E-10	1.280E-08	5.086E-02	5.132E-02	2.279E+00	2.298E+00
ΣH_2S	1.481E-09	1.897E-05	4.938E-04	1.311E-04	9.615E-03	1.150E-02
Mg	2.745E-04	1.805E-05	4.225E-09	1.067E-09	9.871E-04	6.328E-04
Ca	5.026E-02	4.401E-02	4.269E-07	1.619E-07	1.463E-01	5.239E-02
Al	3.416E-06	9.674E-06	9.627E-03	5.250E-03	3.183E-05	8.795E-05
Si	1.177E-03	2.514E-04	1.429E-02	7.450E-02	7.333E-02	4.904E-02
Na	4.997E-01	5.015E-01	6.342E-01	7.033E-01	7.856E-01	9.864E-01
ΣSO_4	1.051E-02	7.004E-03	1.796E-23	1.637E-23	8.390E-20	1.376E-19
Cl	5.620E-01	5.636E-01	6.035E-01	5.991E-01	1.100E+00	1.110E+00
Fe	6.395E-08	1.036E-08	1.536E-08	8.636E-08	6.237E-03	3.555E-03
Cu	6.540E-09	5.456E-10	3.794E-08	2.531E-09	3.917E-03	3.644E-03
Zn	2.542E-06	2.099E-10	2.168E-09	8.545E-08	1.735E-03	3.160E-03
Pb	2.142E-08	1.049E-11	6.741E-11	8.625E-10	1.148E-04	1.891E-04
pH	6.932	7.914	8.757	9.299	4.550	4.683

The peculiar geochemical feature of hydrothermal fluid from the high-temperature root zone consisting of gabbro–peridotite association is its prominent enrichment in the ore elements and significantly lower pH values relative to the starting fluid.

The comparison of composition of modified fluid from the root zones consisting of gabbro–peridotite association with that of peridotite composition leads us to draw the following conclusions. In the low-temperature root zone, fluid obtained by interaction with gabbro differs from fluid that interacted with peridotite in the higher contents of SO_4, H_2S, Al, Si, and lower contents of CH_4, Mg, Fe, Cu, Zn, and Pb. In the moderate–low-temperature root zone, the fluids of the "gabbro" system have the lower contents of CO_2, SO_4, H_2S, Mg, Ca, and Fe and higher contents of Al and Si. The differences in the contents of ore elements in two considered types of fluid for this root zone are insignificant, except for weak decrease in Zn and Pb contents in fluid equilibrium with ophitic gabbro and Cu content in the Fe–Ti gabbro. The composition of model fluid in the high-temperature gabbro–peridotite root zone sharply differs from that from the same root zone consisting of peridotites in significantly higher contents of ore elements.

Discharge Zone

Hydrothermal system with root zone A ($T = 500°C$, $P = 4$ kbar).

When outpouring from the vent on the seafloor surface, the hydrothermal fluid from this root zone due to adiabatic cooling has a temperature of 365°C (Table 4).

Fluid evolution and mineral formation in the feeder channels

Calculations showed that ascent of 1 kg fluid associated with ophitic gabbro in the high-temperature hydrothermal system leads to the release of 0.14 mole gas, while fluid that interacted with Fe–Ti gabbro released 0.16 mole gas (18.2 cm^3 and 21.2 cm^3 at a pressure of 400 bar, respectively). In both cases, gas consisted of predominant hydrogen (70%) and aqueous vapor (30%). The comparison of modeling data with previously obtained results on adiabatic cooling of fluid associated with peridotite (0.08 mole gas or 10.9 cm^3 at a pressure of 400 kbar) showed that the presence of gabbro in the section of high-temperature hydrothermal system provides two times increase of degassing of ascending fluid, at unchanged qualitative composition of gas phase.

The fluid ascent from reaction zone made up of ophitic gabbro is accompanied by the precipitation of predominant quartz, as well as daphnite and chalcosine (Table 5). For high-temperature hydrothermal system with Fe–Ti gabbro in the root zone, the transport of fluid to the surface is accompanied by the precipitation of predominant quartz, as well as albite and chalcosine. Both the mineral assemblages could be considered as assemblages that typically precipitate on the walls of the feeder channels in high-temperature

Table 4. Variations in the chemical composition of hydrothermal fluid during its adiabatic cooling, mol/kg of H_2O

Components	107 (84*)		151 (122)		500 (365)	
	gabbro	Fe-Ti gabbro	gabbro	Fe-Ti gabbro	gabbro	Fe-Ti gabbro
ΣCO_2	1.678E-05	1.050E-05	1.860E-19	7.297E-19	3.185E-14	3.183E-14
CH_4	1.39E-12		2.767E-05	2.811E-05	5.191E-05	5.212E-05
H_2	5.69E-09		5.108E-02	5.163E-02	2.184E+00	2.188E+00
ΣH_2S	3.103E-04		4.938E-04	1.311E-04	9.389E-03	1.056E-02
Mg	9.637E-05	5.366E-06	3.148E-09	2.260E-10	9.871E-04	6.329E-04
Ca	5.026E-02	4.400E-02	2.855E-07	1.616E-07	1.463E-01	5.239E-02
Al	9.120E-09	2.884E-06	5.416E-03	1.190E-06	5.865E-07	3.965E-07
Si	8.327E-04	2.209E-04	1.658E-03	5.875E-02	1.759E-02	1.761E-02
Na	4.997E-01	5.015E-01	6.300E-01	6.981E-01	7.856E-01	9.863E-01
ΣSO_4	1.055E-02	7.149E-03	2.382E-24	1.302E-24	5.706E-23	9.971E-24
Cl	5.620E-01	5.636E-01	6.035E-01	5.991E-01	1.100E+00	1.110E+00
Fe	2.000E-12	1.040E-10	1.535E-08	8.636E-08	6.159E-03	3.557E-03
Cu	6.530E-09	5.310E-10	4.516E-09	1.318E-09	3.663E-03	2.609E-03
Zn	1.000E-12	2.010E-10	1.985E-09	3.954E-08	1.735E-03	3.160E-03
Pb	3.300E-11	2.000E-12	2.200E-11	3.060E-10	1.148E-04	1.891E-04
pH	7.324	8.395	9.803	10.129	4.579	4.244

Note: Here and in Table 5: temperature of hydrothermal fluid after adiabatic cooling.

Table 5. Mineralogy of feeder channels, cm^3/kg of H_2 in fluid

Minerals	107 (84)		151 (122)		500 (365)	
	gabbro	Fe-Ti gabbro	gabbro	Fe-Ti gabbro	gabbro	Fe-Ti gabbro
Albite	0.000342		0.422143	0.526222		0.00859
Galena	6.74E-07			1.57E-08		
Daphnite					0.003334	
Quartz	0.002195				1.263741	0.707233
Pyrite	1.53E-06					
Prehnite		0.000475				
Sphalerite	6.06E-05		4.77E-09	1.09E-06		
Talc	0.00809					
Tremolite		0.000693				
Chalcosine			4.59E-07	1.65E-08	0.003482	0.013965
Epidote		1.42E-06				

hydrothermal system. The main difference in mineralogy of the feeder channels between the upwelling limbs above two considered types of root zones is the presence of albite in the system with Fe–Ti gabbro.

Fluid evolution and mineral formation in the discharge zone

As in (Silantyev et al., 2009b), a mixing of hydrothermal fluid with seawater in the discharge zone was simulated as a series of successive additions of gradually increasing seawater portions to fluid, which was accompanied by the decrease of mixture temperature. The minerals crystallizing during each of the mixing stages and gases released from fluid were removed from the system. The composition of hydrothermal fluid was modified during to adiabatic cooling and coming to the discharge zone (Table 4).

At the initial stage of mixing of hydrothermal fluid of both these types with seawater, the released gas phase is qualitatively and quantitatively identical to

the composition obtained by mixing of seawater with peridotite-related fluid. In the first reactor, 1 kg of diluted fluid at temperature of 329°C and seawater faction of 0.1 yielded 0.63 mole gas (79.5 cm^3 at pressure of 400 bar) consisting mainly of hydrogen (70%) and aqueous vapor (30%). The gas phase also contains H_2S (0.07%) and methane (0.01%). Increase in seawater content with subsequent mixing results in the decrease of total volume of released gas up to 0.007 mole (0.66 cm^3 at a pressure of 400 bar) at temperature of 177°C and seawater fraction of 0.52. Hydrogen and methane fractions in the gas phase gradually increase (97% and 0.33% in the reactor, respectively, at temperature of 177°C), whereas volume of released H_2S remains practically unchanged. No degassing is observed during subsequent mixing.

In the discharge zone of high-temperature hydrothermal fluid that supplied to the seafloor from the root zones made up of ophitic or Fe–Ti gabbro, following sequence of minerals is precipitated in the course of its mixing with seawater and corresponding decrease of temperature of this mixture (Figs. 3a, 3b):

T = 330–220°C (seawater fraction of 0.1–0.45): *Bn* + *Sp* + *Gn* + *Ccp* + *Po* + *Qtz* + *Tlc* + *Chl* (*Dph*);

T = 220–25°C (seawater fraction of 0.45–0.90): *Po* + *Ccp* (traces remain at 90°) + *Gn* (traces) + *Ctl* + *Brc* + Ca-*Sap* (appears at 50°C) + *Chl* (traces);

T = 25–5°C (seawater fraction of 0.90–0.99): *Py* + Ca-*Sap* + *Dol*.

Calculation results showed that intense precipitation of sulfides during mixing with high-temperature fluid (up to seawater fraction of 0.90) is provided by the high contents of H_2S and H_2, which determine the reduction of sulfide ion from seawater. In spite of the hydrogen consumption for reduction, mixing was accompanied by its release into gas phase, which is related to the decrease of H_2 solubility with decreasing temperature.

The predominant part of ore material represented by sphalerite, galena, pyrrhotite, chalcopyrite, chalcosine, and bornite is precipitated from the high-temperature hydrothermal fluid in the course of its mixing with seawater at temperature of 330–175°C and seawater fraction of 0.1–0.5 (Figs. 4a, 4b). At this stage of mixing, the high-temperature fluid losses practically all ore elements. Pyrite appears in the model ore edifice only at the final stages of fluid–seawater mixing at temperature about 50°C and seawater fraction more than 0.85. Fig. 4a demonstrates the sequence of ore formation in a narrow range of conditions corresponding to temperatures of 362–271°C and seawater faction 0.01–0.25. The sequence of precipitation of ore phases during "slow" mixing of fluid with seawater in the high-temperature region of the system is bornite + chalcosine ⟶ galena + pyrrhotite + sphalerite + bornite (normal gabbro) (Fig. 4a); bornite + sphalerite ⟶ galena + pyrrhotite + sphalerite + bornite (Fe–Ti gabbro) (Fig. 4b).

In the low-temperature mixing field (seawater fraction > 0.90) with pyrite as single precipitating sulfide phase, hydrothermal fluid in physical-chemical aspect becomes indistinguishable from seawater.

The above data revealed significant differences between processes of mineral formation at the downwelling limb of hydrothermal systems with high-temperature root zone consisting of different types of crustal protolith: gabbros and peridotites. Vein complex related to the feeder channels of this reaction zone made up of Fe–Ti gabbro includes leucocratic rocks consisting of quartz and albite. Feeder channels above the reaction zone represented by ophitic gabbro are made up of quartz with sharply subordinate chlorite. For both the types of reaction zone, the ore phase in the feeder channels is represented by chalcosine. In the peridotite scenario of simulation of high-temperature hydrothermal system (Silantyev et al., 2009b), the feeder channels are represented by distinct mineral assemblage: quartz + daphnite + talc + pyrrhotite. Ore assemblage of hydrothermal edifices produced by discharge of high-temperature fluid ascending from the root zone made up of normal or Fe–Ti gabbro differs from the ore assemblage of high-temperature discharge zone of fluid that separated from peridotite hydrothermal reactor in the presence of significant amount of galena.

Hydrothermal system with root zone (T = 151°C, P = 1.4 kbar).

For this root zone, hydrothermal fluid outpouring from feeder channel due to adiabatic cooling has a temperature of 122°C.

Evolution of fluid and mineral formation in the feeder channels

The ascent of both types of fluid associated with gabbro in the moderate–low-temperature hydrothermal system showed no degassing, like fluid that was formed during interaction with peridotite protolith.

In the root zone represented by ophitic gabbro, fluid crystallizes albite (predominant), sphalerite, and chalcosine (Table 5). In the feeder channels located above moderate–low-temperature root zone consisting of Fe–Ti gabbro, this mineral assemblage is supplemented by galena. Since concentrations of ore elements in moderate–low-temperature fluid is extremely low, the volume of ore phases during its adiabatic expansion is insignificant, being lower than their content in mineral assemblage of feeder channels in the high-temperature hydrothermal system.

Fluid evolution and mineral formation in the discharge zone

Moderate–low-temperature hydrothermal system differs from the high-temperature zone in terms of pH evolution of hydrothermal fluid during its mixing with

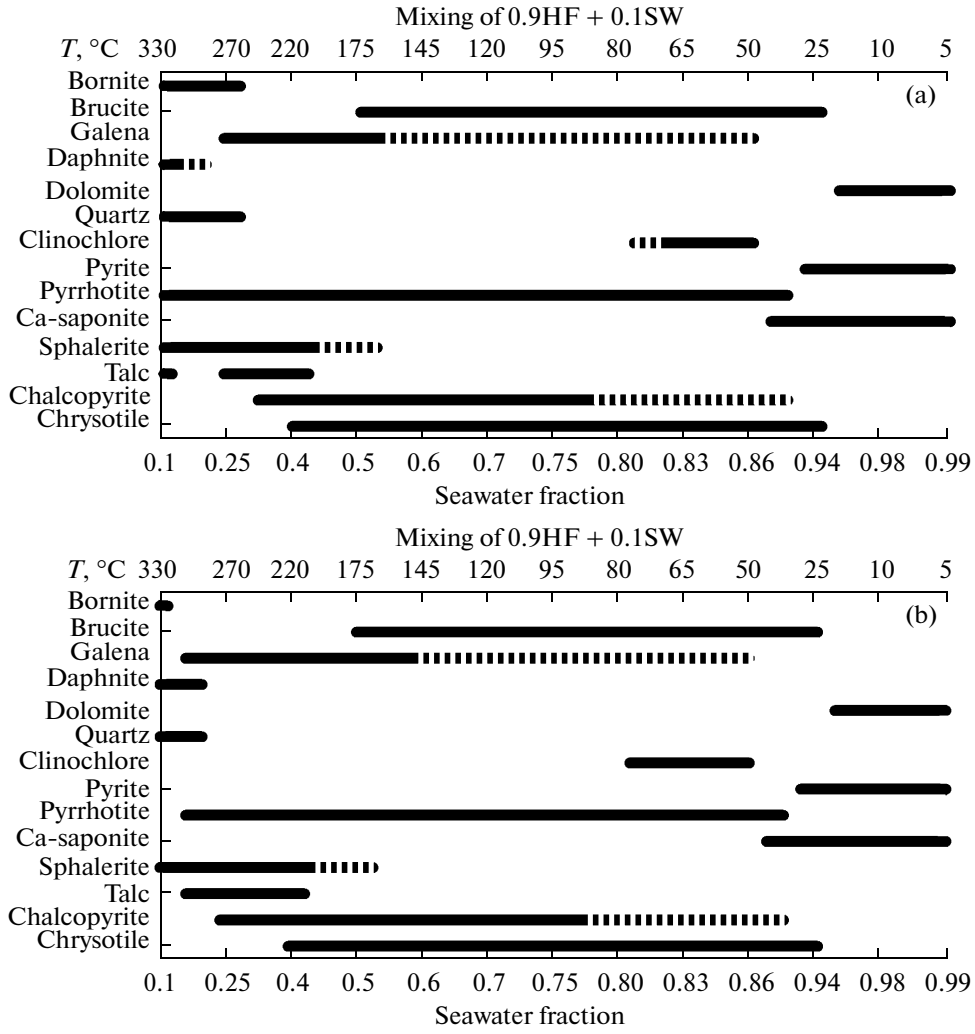

Fig. 3. Sequence of mineral precipitation from hydrothermal fluid that supplied to the discharge zone from the high-temperature gabbro root zone, (scenario A) during its mixing with seawater. (a) ophitic gabbro, (b) Fe–Ti gabbro. For Figs. 3–6: (HF) hydrothermal fluid, (SW) seawater.

seawater. Within a temperature range of 110–60°C, pH sharply decreases from 9.8 to 7.

In the discharge zone of moderate–low-temperature fluid, the processes of mineral formation significantly differ from those obtained by calculations for high-temperature system. A gradual mixing of fluid with seawater and decrease of temperature lead to the formation of the following sequence of mineral precipitation (Figs. 5a, 5b):

$T = 110–90$°C (seawater fraction of 0.1–0.30)

Ophitic gabbros: *Brc* (predominant) + *Chl* (daphnite) + *Po* + *Sp* (trace amounts) + *Ccp* (trace amounts);

Fe–Ti gabbros: *Ctl* + *Chl* (daphnite) + *Tlc* + *Tr* + *Sp* (trace amounts) + *Gn* (trace amounts);

$T = 90–20$°C (seawater fraction of 0.30–0.86).

Ophitic gabbro: *Dol* + *Chl* (clinochlore) (disappears at 60°C) + Ca-*Sap* + *Py*;

Fe–Ti gabbro: *Dol* + Ca-*Sap* + *Py* + *Ctl* (disappears at 65°C) + *Tlc* (disappears at 60°C) + *Tr* (disappears at 75°C).

$T = 20–5$°C (seawater fraction of 0.86–0.99).

For both petrographic types of gabbro: Ca-*Sap* + *Py* + *Dol*.

Since the contents of ore elements in the discharge zone of moderate–low-temperature fluid that separated from gabbroid reactors of both types are extremely low, its mixing with seawater does not lead to the precipitation of significant amounts of sulfides. Therefore, the hydrothermal edifices in this case are mainly made up of barren phases.

An important feature of moderate–low-temperature hydrothermal system with the gabbro root zone is inherent sulfide mineralization in the feeders of upwelling limb. This feature differs the moderate–low-temperature circulation systems related with gab-

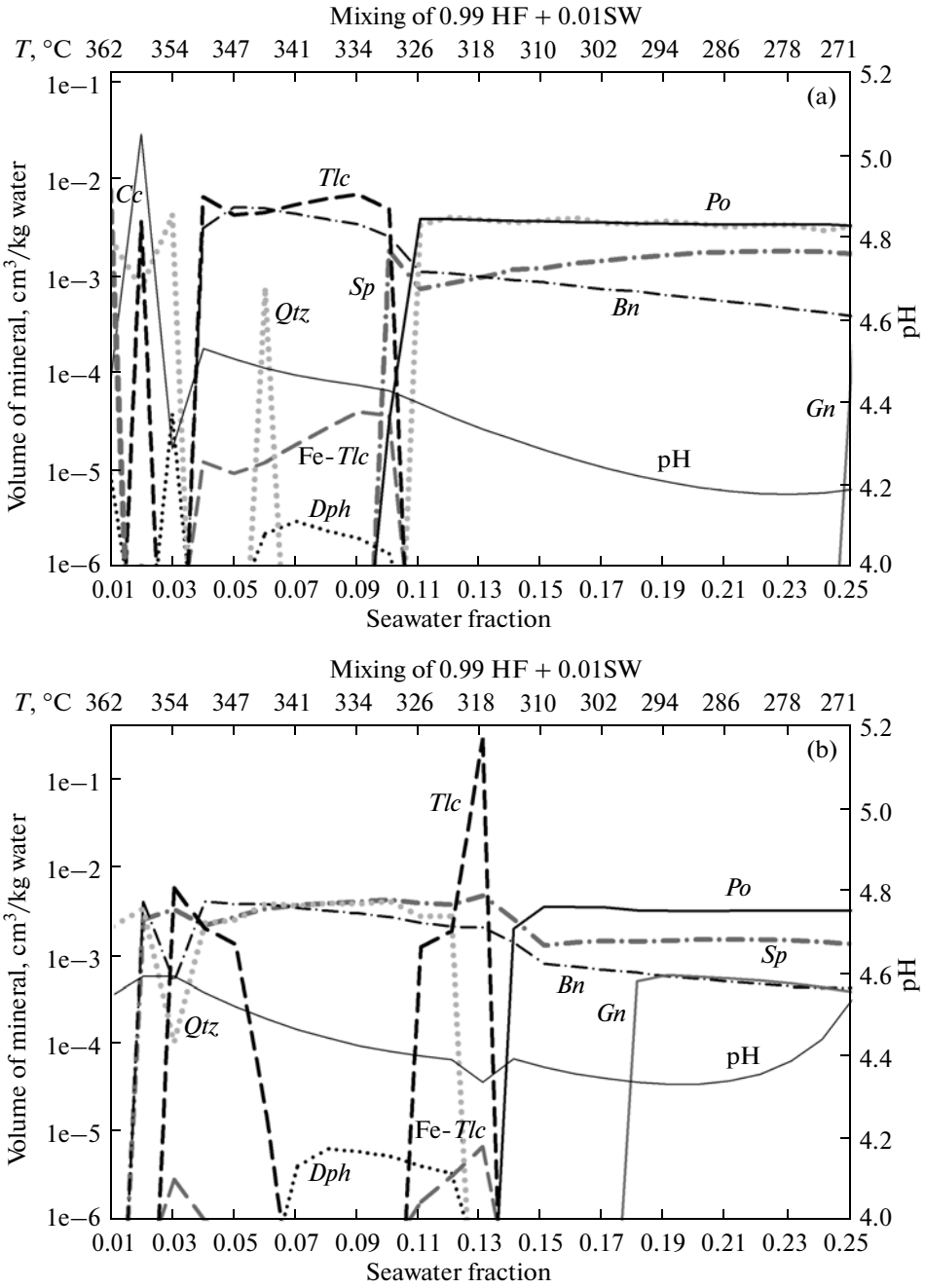

Fig. 4. Sequence of mineral precipitation from the hydrothermal fluid that percolated to the discharge zone from the high-temperature gabbro root zone (scenario A), during its mixing with seawater at temperature of 330°–175°C and seawater fraction of 0.1–0.5. (a) ophitic gabbro, (b) Fe–Ti gabbro.

bro from their analogues related to the peridotite hydrothermal reactor.

Hydrothermal system with root zone C (T = 107°C, P = 1.14 kbar).

In the mouth of feeder channel, hydrothermal fluid had a temperature of 84°C.

Computer simulation of the low-temperature system revealed that mineral formation in the fluid-feeder channel resembles those calculated for moderate–low-temperature system. At the upwelling limb of the low-temperature system with root zone made up of ophitic gabbros, fluid precipitates the following mineral assemblage: albite + quartz + talc (predominant) + sphalerite + pyrite + galena (Table 5). Fluid transported to the seafloor surface from the root zone consisting of Fe–Ti gabbro crystallizes only silicate phases: prehnite + tremolite + epidote (traces).

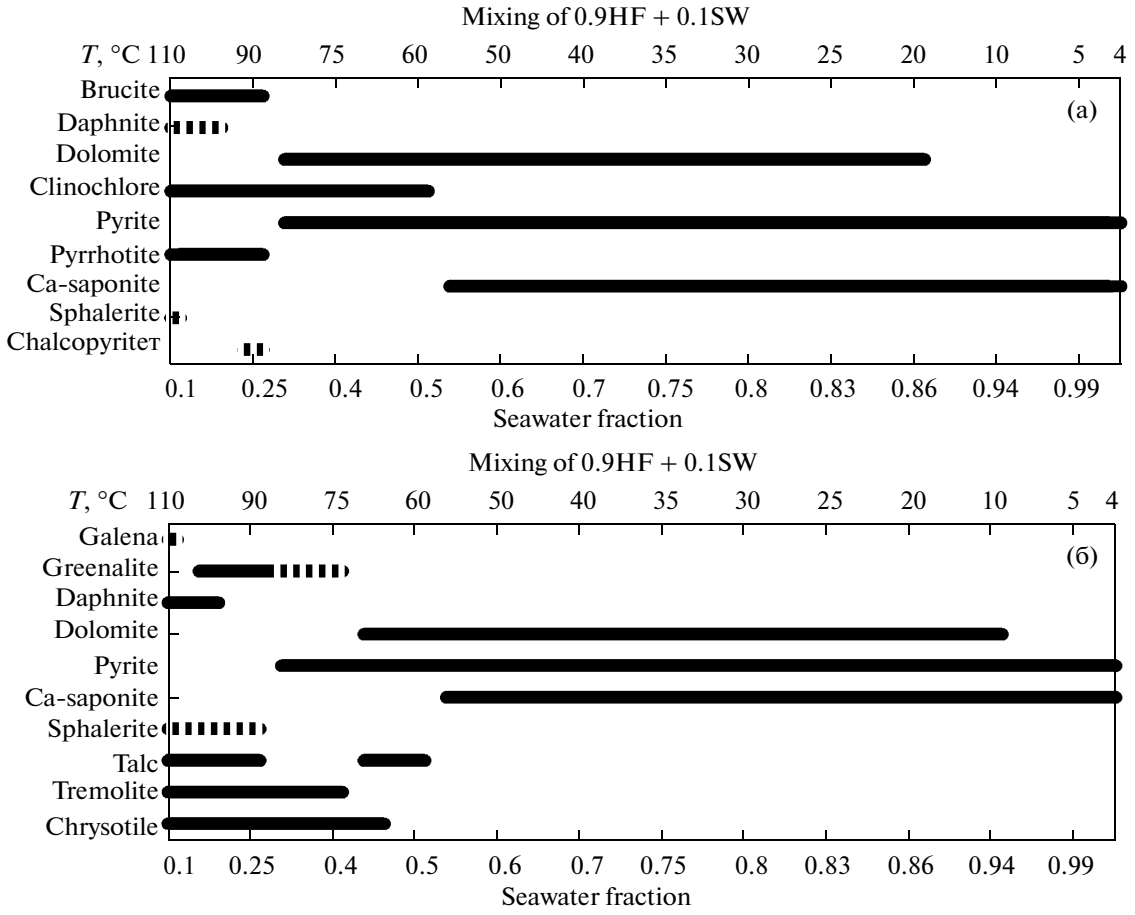

Fig. 5. Sequence of mineral precipitation from the hydrothermal fluid that supplied to the discharge zone from the moderate–low-temperature gabbro root zone, during its mixing with seawater. (a) ophitic gabbro, (b) Fe–Ti gabbro.

With decrease of temperature and increase of seawater fraction, the pH value in the low-temperature discharge zone changes insignificantly within 6.6–6.8 in the ophitic gabbro and more significantly within 7.3–6.8 in the Fe–Ti gabbro. In the discharge zone of the upwelling limb on the seafloor surface, the low-temperature hydrothermal fluid is depleted in Mg and Fe relative to seawater. During mixing with seawater, fluid rapidly losses H_2S and H_2 (practically completely while reaching 25°C and seawater fraction of 0.78) against the background of increase of CO_2 content. No degassing is observed in the hydrothermal fluid during its ascent to the seafloor surface and mixing with seawater.

In the hydrothermal source related to the low-temperature root zone (regardless of the petrographic type of the constituent gabbro), two mineral assemblages are subsequently precipitated from fluid during its mixing with seawater (Figs. 6a, 6b):

(1) $T = 75–60$°C (seawater fraction of 0.1–0.27)

Ophitic gabbros: *Ab* + *Qtz* + *Tlc* + *Py*;

Fe–Ti gabbro: *Dol* + *Hem* + *Tlc* + *Chl*;

(2) $T = 60–5$°C (seawater fraction of 0.34–1.0).

Ophitic gabbros: *Qtz* + *Dol* + Ca-*Sap* + *Py* + *Gt* + *Cv* (trace amounts);

Fe–Ti gabbro: *Dol* + *Gt* + Ca-*Sap*.

As for moderate–low-temperature system, the peculiar feature of mineral formation at the upwelling limb of low-temperature hydrothermal system with gabbroic root zone is sulfide mineralization in the feeder channels. However, the ore assemblage in this scenario of hydrothermal circulation lacks chalcosine.

Precipitation from pure seawater at its heating near hydrothermal spring

Previously obtained results of numerical simulation (Silantyev et al., 2009b) showed that seawater heating provides the successive crystallization of the following mineral phases: dolomite + goethite + Ca-saponite + pyrite ⟶ anhydrite + magnesite (predominant) + hematite + calcite ⟶ anhydrite + brucite (predominant) + antigorite + hematite + chlorite. It can be taken that assemblage saponite + pyrite + dolomite simulated at high seawater/fluid ratios and low temperatures is formed by precipitation of miner-

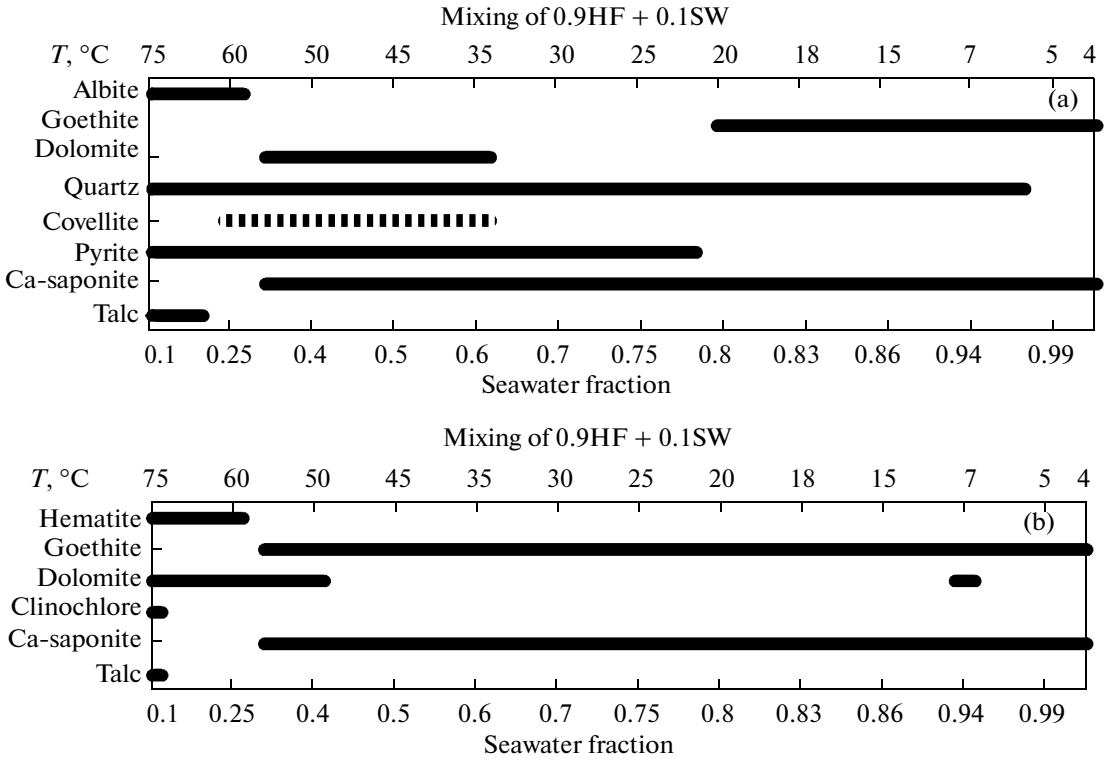

Fig. 6. Sequence of mineral precipitation from the hydrothermal fluid that supplied to the discharge zone from the low-temperature gabbro root zone during its mixing with seawater. (a) ophitic gabbro, (b) Fe–Ti gabbro

als from pure seawater during its heating near hydrothermal spring.

Thus, the transport of hydrothermal fluid separating from low-temperature hydrothermal gabbroid reactor to the seafloor surface is accompanied by precipitation of most part of ore material in the feeder channel. In this scenario, ore edifices in the fluid discharge zones are either absent or made up of weakly consolidated diffuser-type deposits. Obviously, the main factor responsible for the rapid precipitation of ore material from the gabbro-related fluid is its higher (as compared to peridotite-related fluid) oxidizing potential. Fluid formed in the high-temperature root zone is able to transfer into discharge zone significantly greater amounts of ore components, whose precipitation during mixing with seawater leads to the formation of ore edifices. It is noteworthy that unlike ore occurrences related to the peridotite reactor, the gabbro-related ore mineral assemblage is dominated by galena.

MODEL VERIFICATION AND ESTIMATION OF GABBRO ROLE IN THE MATERIAL BALANCE DURING HYDROTHERMAL TRANSFORMATON OF THE CRUSTAL PROTOLITH OF SLOW-SPREADING RIDGES

Data obtained by our simulation make it possible, on the one hand, to interpret the diversity of mineral types of metagabbroids observed in the slow-spreading MOR in the framework of the existing models of hydrothermal systems operating in the Hess-type oceanic crust. On the other hand, revealed geochemical and mineralogical effects related to the transportation of hydrothermal fluid that separated from different-depth root zones consisting of gabbroids enable estimation of the role of gabbro in the material balance during hydrothermal transformation of the crustal protolith of slow-spreading ridges.

Mineralogy of the root zones

Three mineral assemblages were simulated for three different-depth root zones forming in the ophitic (normal) and Fe–Ti gabbro during interaction with hydrothermal fluid that percolated through peridotite section. These assemblages correspond to the mineral types of oceanic metagabbros (for instance, Gillis, 1993; Silantyev, 1995, 1998) and indicator mineral assemblage of the facies grid of the low–moderate-temperature metamorphism of the basic rocks in the NCMASH system (Liou et al., 1985; Bevins and Robinson, 1993). In Fig. 7, the obtained mineral assemblages are situated in the stability fields of the zeolite (root zones C and B) and lower amphibolite (root zone A) facies. Secondary minerals of the gabbroids from the moderate–low temperature and high temperature root zones form assemblages that are typical

of metagabbros from the well-known MAR segments, for instance, 23°N (MARK): actinolite + chlorite ± talc ± epidote ± prehnite ± titanite (Fletcher et al., 1997); 13°–17°N: pargasite + Al-actinolite + chlorite + plagioclase (*An* < 30) + titanite (Silantyev, 1998). The formation of Fe-chlorite, Fe-actinolite, and Fe-pargasite in the high-temperature root zone corresponds to the experimentally established phenomenon of increasing iron mole fraction in the coexisting amphibole and chlorite from the metabasic rocks of the oceanic hydrothermal systems with decreasing W/R ratio (Mottl, 1983). In the high-temperature scenario of the considered model, the low W/R ratio is provided by the short residence time of fluid in the hydrothermal reactor. Calculated data, as was noted above, reproduced mineral variations of gabbro under the zeolite-facies conditions (107–151°C), which were reconstructed previously empirically and experimentally (Liou et al., 1983, 1991; Fridriksson et al., 2001; Digel and Ghent, 2007): enrichment of stilbite in stellerite end member; the replacement of stilbite by lomontite with increasing temperature; and the change of epidote by clinozoisite. Data obtained during modeling indicate that the ore mineralization in the gabbros of root zones is preferentially developed in the low-temperature systems, whereas gabbroids of high-temperature root zones are characterized by the almost complete absence of secondary ore phases.

Simulated mineral types of gabbroids are widespread in the MAR crest zone (for instance, Gillis et al., 1993; Silantyev, 1998; Fletcher et al., 1997), where they compose the oceanic core complexes, including those hosting large hydrothermal fields (Ashadze, Logachev, Rainbow).

Compositional Evolution of Gabbros in the Root Zone of Hydrothermal System

Empirical data (Silantyev, 1995, 1998) indicate that metamorphism of MOR gabbroids is characterized by the mobile behavior of most major elements. As was noted above, the results of numerical simulation showed that the strongest major-element alterations of both the considered petrographic types of gabbros during their interaction with fluid, regardless of their starting composition, are observed in the highest temperature root zone. The latter, according to the calculations, demonstrates the same geochemical effects, which were previously established by studying the natural objects and consist in the removal of calcium, aluminum, silica, magnesium, and iron from gabbroids. Thus, the behavior of major elements during high-temperature transformation of gabbros in the root zones of hydrothermal systems is controlled by major geochemical trends of oceanic metamorphism. One of the important modeling results is the established effect of intense removal of Cu, Zn, and Pb from gabbro in the high-temperature reaction zone. This effect highlights the different-scale mobilization of ore material in the root zones of hydrothermal systems made up of peridotites or gabbros.

Numerical reconstruction of mineral and chemical transformations in the gabbroids from the root zones of hydrothermal systems of slow-spreading MAR leads us to conclude that the observed mineral and geochemical diversity of metagabbros in the modern oceanic basins was provided by interaction of gabbro with hydrothermal fluid that percolated through peridotite section of the Hess-type oceanic crust.

Mineralogy of Feeder Channels and Vein Complex

Presented above data indicate significant mineralogical differences between vein complexes that were formed during fluid transport from root zones consisting of different types of crustal protolith: gabbros or peridotites. Indicator phases for feeder channels located above gabbroid root zones are albite, galena, and chalcosine associated with talc, chlorite, and tremolite. In contrast, the feeder channels above "peridotite" root zone are made up of different mineral assemblage: quartz + pyrrhotite + chlorite + talc (Silantyev et al., 2009b). Obtained results enable us to state that the peculiar feature of low-temperature hydrothermal systems with the gabbro root zone is inherent sulfide mineralization in the feeder channels of upwelling limb. Such mineralization is absent in the vein complex of low-temperature circulation systems related to the peridotite hydrothermal reactor (Silantyev et al., 2009a).

It should be noted that the albite + quartz + talc + tremolite assemblage was also established in the hydrothermal veins of oceanic core complexes containing gabbroids in many areas of the MAR axial zone: 15°37′N and 16°52′N (Cannat et al., 1992); 23°N (Caggero and Cortesogno, 1997); 30°N (*Expedition...*, 2006). According to (D'Orazio et al., 2004; Bach and Klein, 2007), an ubiquitous presence of talc (often in association with albite and quartz) in the aforementioned objects indicates the high silica activity in fluid, which is confirmed by the above calculations.

Summing up the data on mineralogy of feeder channels and vein complex of hydrothermal systems with gabbro root zone, the conclusion may be drawn that the ascent of hydrothermal fluid that separated from low-temperature hydrothermal reactor to the seafloor surface is accompanied by precipitation of most part of ore material in the feeder channel.

Processes in the Discharge Zone

The simulated sequence of mineral formation (bornite + chalcosine + sphalerite ⟶ galena + pyrrhotite + sphalerite + bornite) in the discharge zone of high-temperature hydrothermal fluid (365°C) during its mixing with seawater resembles zoning observed in the ore edifices of high-temperature MAR hydrothermal fields

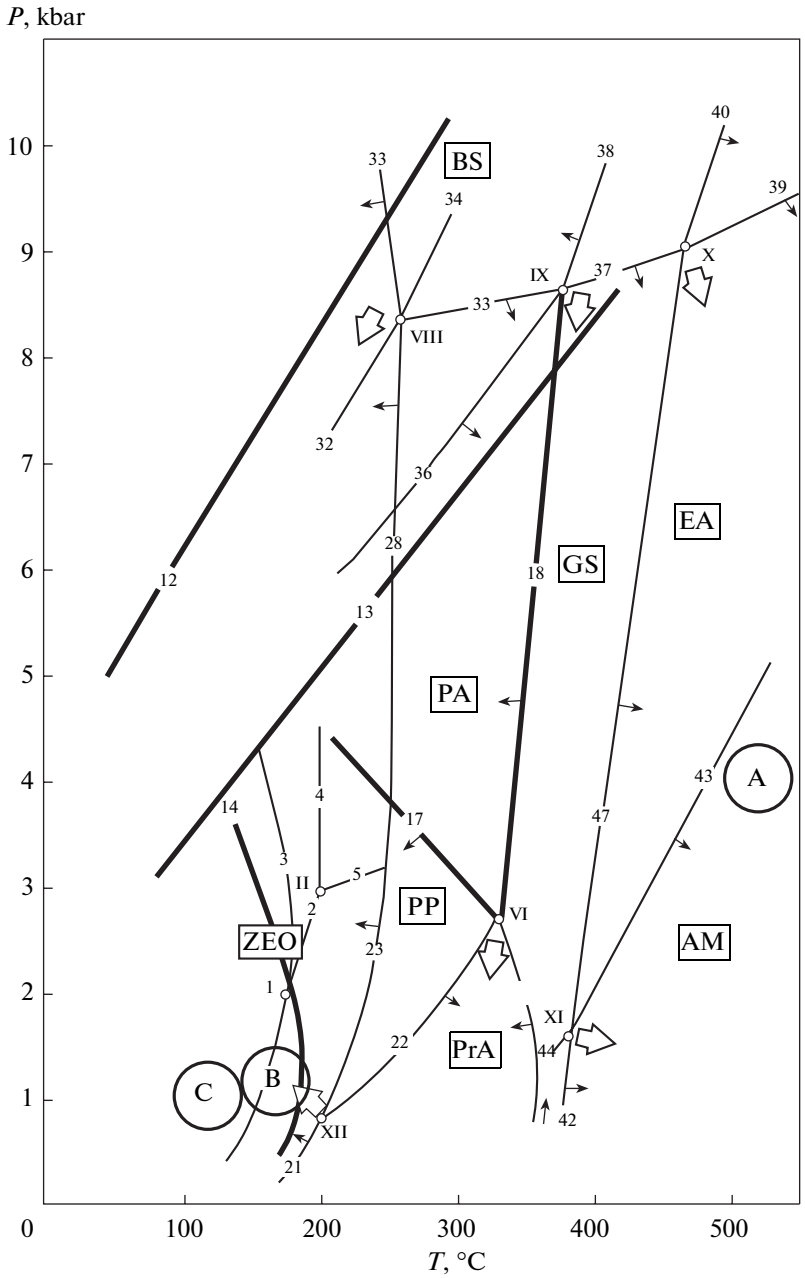

Fig. 7. *P–T* diagram of the low-grade metamorphic facies of basic rocks (NMASH system) according to (Liou et al., 1985; Bevins and Robinson, 1993). Metamorphic facies: (BS) blueschist, (EA) epidote–amphibolite, (AM) amphibolite, (GS) green schist, (PA) pumpellyite–actinolite, (PP) prehnite–pumpellyite, (PrA) prehnite–actinolite, (ZEO) zeolite. Fields of simulated gabbroid mineral assemblages after their interaction with hydrothermal fluid in high-temperature (A), moderate–low temperature (B), and low-temperature (C) root zones.

associated with serpentinized peridotites: Ashadze and Logachev (sphalerite + Cu–Fe-sulfides ⟶ pyrrhotite + chalcopyrite + sphalerite) (Shipboard..., 2007). The model sulfide assemblage from high-temperature hydrothermal system with gabbroid root zone is also close to the ore assemblage observed in the active sulfide edifices of the Rainbow hydrothermal field (chalcopyrite + sphalerite + bornite + cubanite) (Vikent'ev, 2004). However, judging from modeling results, the only and significant difference of the ore edifices of high-temperature hydrothermal systems with gabbroid root zones from those of peridotite root zones is the notable presence of galena.

As was noted above, the mixing of moderate–low temperature and low temperature fluids with low contents of ore components in the discharge zone with seawater provides the formation of barren hydrothermal edifices. The mineralogy of these barren com-

plexes is represented by brucite, chlorite, talc (at the initial stages of mixing) and dolomite, saponite, pyrite and hematite (at the final stages of mixing at $T \leq 75°C$). Saponite–goethite–pyrite mineral assemblage is typical of the hydrothermal precipitates surrounding the active hydrothermal fields of the Central Atlantic (Silantyev et al., 2009a). Therefore, there are grounds to assume that the geochemical and mineralogical effects determinable by fluid mixing in the low-temperature hydrothermal systems of the Hess-type crust do not depend on the rock type that composes their root zones: gabbros or peridotites.

Model calculations showed that fluid that was supplied to the discharge zone from the high-temperature hydrothermal gabbro reactor is practically identical to the hydrothermal fluid related to the peridotite root zone in terms of contents of dissolved gases, cations (Mg, Ca, Si, Na) and pH level. However, it has significantly higher contents of ore components: Cu, Zn, and Pb. It should be particularly noted that the high lead contents established during modeling in high temperature hydrothermal fluid derived from the gabbroic root zone are not typical of the fluid composition in the discharge zones of known hydrothermal systems of MAR located in serpentinites (for instance, Tivey, 2007). Simulation results showed that fluid transported in the discharge zone from the low-temperature gabbroic root zones, unlike fluids of peridotite system, reveals the lower contents of CH_4, H_2, H_2S, Mg, Fe, and all ore elements.

Role of Gabbro in the Material Balance during Hydrothermal Process in Slow-Spreading MAR

Results of simulations presented in this paper provide new insight in some problems of material balance and ore formation during hydrothermal process in the slow-spreading MAR.

The comprehensive summary of Herzig and Hannigton (1995) dedicated to the geochemical typification and geodynamic position of the polymetallic massive sulfide occurrences in the modern oceanic basins indicates that the ore edifices of active hydrothermal fields of oceanic basins are made up of variable proportions of pyrrhotite, sphalerite, chalcopyrite, bornite, isocubanite, and pyrite. The authors also concluded that the oceanic sulfide-polymetallic ore occurrences are characterized by Cu–Zn specialization, which determines the absence of significant amounts of galena in the ore edifices of the MAR hydrothermal fields. This conclusion is supported by the available mineralogical data on the ore edifices of the MAR hydrothermal field located in serpentinites: Ashadze and Logachev (*Shipboard...*, 2007); Semenov field (Beltenev et al., 2009), and Rainbow field (Vikent'ev, 2004).

Taking into account the aforementioned facts, our simulation data on the ubiquitous presence of galena in the mineral assemblage of ore edifices in the fluid discharge zone can be interpreted as indicating the absence of gabbroids in the high-temperature root zones of presently known MAR hydrothermal systems related to serpentinites. This indicates that the root zones in all these hydrothermal fields are made up of peridotites. It is highly possible that the main role of gabbroids in the deepest seated root zones is to supply heat for hydrothermal circulation system. One can suggest that the root zones in the aforementioned hydrothermal fields of MAR are hosted by peridotite protolith near the hot or uncooled gabbroic bodies.

In contrast to data obtained for high-temperature systems, trends simulated for material balance and mineral formation in the low-temperature hydrothermal systems with gabbroid root zones possibly take place on natural objects. This can be confirmed by the wide development of hydrothermal veins consisting of albite + quartz + talc + tremolite assemblage in the oceanic core complexes of MAR. The precipitation of this assemblage in the feeder channel was simulated during adiabatic cooling of low-temperature hydrothermal fluid. It is worthy to remind that the most part of ore material transferred by hydrothermal fluid from the low-temperature hydrothermal gabbro reactors to the seafloor surface is precipitated in the feeder channel. Thus, almost cooled gabbroid bodies, being involved in the hydrothermal circulation in shallow-depth root zones, may play an important role in redistribution of the material within the Hess-type oceanic crust.

Mineral and chemical transformations established in the gabbroids of root zones of hydrothermal systems of slow-spreading MOR allow us to state that the observed mineral and geochemical diversity of metagabbros of modern oceanic basins can be produced by interaction of gabbro with hydrothermal fluid percolating through peridotite section of the Hess-type oceanic crust.

Simulation of hydrothermal system hosted in the serpentinites with gabbro root zone allows us to formulate several conclusions concerning the role of gabbro in the material balance during hydrothermal transformation of crustal protolith of slow-spreading ridges.

(1) Root zones of all known MAR hydrothermal fields related to serpentinites are made up of ultrabasic rocks and located within the peridotite protolith near hot or uncooled gabbroic bodies.

(2) The observed mineral and geochemical diversity of metagabbros of slow-spreading MOR can be provided by interaction of hydrothermal fluid that percolated through peridotite section of the Hess crust with gabbroic bodies.

(3) Vein complex of feeder channels of low-temperature hydrothermal systems with gabbroid root zones can be considered as potential concentrators of ore matter in the oceanic crust section consisting of gabbro–peridotite association.

(4) The low-temperature hydrothermal systems with gabbroid root zones are not promising for search of hydrothermal occurrences on the seafloor surface.

(5) Quartz + albite assemblage in the hydrothermal vein complex of peridotites of slow-spreading MAR can be considered as indicator of gabbroid reaction zones of hydrothermal systems made up of gabbroids.

(6) The trends of material balance observed in the hydrothermal systems with root zones consisting of ophitic gabbros are similar to those observed in the systems with Fe–Ti gabbro root zone.

(7) The interaction of gabbro with marine fluid in the root zone occurs at much lower rates than hydrothermal transformation of peridotite. As a result, the hydrothermal fluid coexisting with gabbro at moderate and low temperatures is able to preserve its oxidizing properties for a long time and determine the deeper location of boundary between zones of sharply oxidizing (fluid-dominant) and moderately oxidizing regime distinguished by (Silantyev et al., 2009a) in the Hess-type crust.

ACKNOWLEDGMENTS

This work was supported by the Russian Foundation for Basic Research (project nos. 09-05-00008 and 08-05-00164a) and Program of Presidium of the Russian Academy of Science "Fundamental Problems of Oceanology: Physics, Geology, Biology, and Ecology" (theme "Interaction of Magmatic and Hydrothermal Systems in the Oceanic Lithosphere and Mineral Resources).

REFERENCES

1. Alt, J.C., Shanks, W.C., Bach, W., Paulick, H., Garrido, C.J., and Beaudoin, G., Hydrothermal Alteration and Microbial Sulfate Reduction in Peridotite and Gabbro Exposed by Detachment Faulting at the Mid-Atlantic Ridge, 15°20′N (ODP Leg 209): A Sulfur and Oxygen Isotope Study, *Geochem. Geophys. Geosyst.*, 2007, vol. 8, p. Q08002. doi:10.1029/2007GC001617.
2. Bach, W. and Klein, F., Silica Metasomatism of Oceanic Serpentinites, in *Goldschmidt Conference Abstracts*, 2007, p. A48.
3. Beltenev, V., Ivanov, V., Rozhdestvenskaya, I., Gustaytis, A., Popova, Ye., Amplieva, Ye., and Evrard, C., New Data on Hydrothermal Fields on the Mid-Atlantic Ridge Between 11°–14°N: 32-nd Cruise of R/V "Professor Logachev", *InterRidge News,* 2009, vol. 18, pp. 13–17.
4. Beltenev, V., Ivanov, V., Shagin, A., Sergeyev, M., Rozhdestvenskaya, I., Shilov, V., Dobretzova, I., Cherkashev, G., Samovarov, M., and Poroshina, I., New Hydrothermal Sites at 13°N, Mid-Atlantic Ridge, *InterRidge News*, 2005, vol. 14, pp. 14–16.
5. Bevins, R. and Robinson, D., Mineral Parageneses in Low-Grade Metabasites at Low Pressures and Consideration of the Sub-Greenschist Realm, *Eur. J. Mineral.*, 1993, vol. 5, pp. 925–935.
6. Cannat, M., Bideau, D., and Bougault, H., Serpentinized Peridotites and Gabbros in the Mid-Atlantic Ridge Axial Valley at 15°37′N and 16°52′N, *Earth Planet. Sci. Lett.*, 1992, vol. 109, pp. 87–106.
7. D'Orazio, M., Boschi, C., and Brunelli, D., Talc-Rich Hydrothermal Rocks from the St. Paul and Conrad Fracture Zones in the Atlantic Ocean, *Eur. J. Mineral*, 2004, vol. 16, no. 1, pp. 73–83.
8. Delacour, A., Früh-Green, G.L., and Bernasconi, S.M., Sulfur Mineralogy and Geochemistry of Serpentinites and Gabbros of the Atlantis Massif (IODP Site U1309), *Geochim. Cosmochim. Acta*, 2008, vol. 72, pp. 5111–5127.
9. Digel, S. and Ghent, E.D., Fluid–Mineral Equilibria in Prehnite–Pumpellyite to Greenschist Facies Metabasites Near Flin Flon, Manitoba, Canada: Implications for Petrogenetic Grids, *J. Metamorph. Geol.*, 2007, vol. 12, no. 4, pp. 467–477.
10. *Expedition 304/305 Scientists, Site U1309*, Blackman, D.K., Ildefonse, B., John, B.E., Ohara, Y. et al., Eds. *Proc. IODP, 304/305*, College Station, TX: Integrated Ocean Drilling Program Management International, 2006.
11. Fletcher, J.M., Christopher, J.., Stephens, C.J., Erich, U.., Petersen, E.H., and Skerl, L., Greenschist Facies Hydrothermal Alteration of Oceanic Gabbros: a Case Study of Element Mobility and Reaction Paths, Karson, J.A., Cannat, M., Miller, D.J., and Elthon, D., Eds., *Proc. Ocean Drill. Progr., Sci. Res.*, 1997, vol. 153, pp. 389–398.
12. Fridriksson, T., Neuhoff, P.S., Arnörsson, S., and Bird, D.K., Geological Constraints on the Thermodynamic Properties of the Stilbite–Stellerite Solid Solution in Low-Grade Metabasalts, *Geochim. Cosmochim. Acta*, 2001, vol. 65, no. 21, pp. 3993–4008.
13. Fujiwara, T., Lin, J., Matsumoto, T., Kelemen, P.B., Tucholke, B.E., and Casey, J., Crustal Evolution of the Mid-Atlantic Ridge Near the Fifteen–Twenty Fracture Zone in the Last 5 Ma, *Geochem. Geophys. Geosyst.*, 2003. doi: 4:10.1029/2002GC000364.
14. Gaggero, L. and Cortesogno, L., Metamorphic Evolution of Oceanic Gabbros: Recrystallization from Subsolidus To Hydrothermal Conditions in the MARK Area (ODP Leg 153), *Lithos*, 1997, vol. 40, nos. 2–4, pp. 105–131.
15. Gillis, K.M., Thompson, G., and Kelley, D.S., A View of the Lower Crustal Component of Hydrothermal Systems at the Mid-Atlantic Ridge, *J. Geophys. Res.*, 1993, vol. 98, no. B11, p. 619.
16. Herzig, P.M. and Hannington, M.D., Polymetallic Massive Sulfides at the Modern Seafloor a Review, *Ore Geol. Rev.*, 1995, vol. 10, no. 2, pp. 95–115.
17. Jambon, A., *Earth Degassing and Large-Scale Geochemical Cycling of Volatile Elements, in Volatiles in Magmas, Rev. Mineral., Carroll, M.R. and Holloway, J.R*, Eds., Washington, DC: Mineral. Soc. Amer., 1994, vol. 30, pp. 479–517.
18. Johnson, J.W., Oelkers, E.H., and Helgeson, H.C., SUPCRT92: A Software Package for Calculating the Standard Molal Thermodynamic Properties of Minerals, Gases, Aqueous Species, and Reactions from 1 to

5000 Bars and 0° to 1000°C, *Comp. Geosci.*, 1992, vol. 18, pp. 899–947.

19. Kelley, D.S. and Delaney, J.R., Two-Phase Separation and Fracturing in Mid-Ocean Ridge Gabbros at Temperatures Greater Than 700°C, *Earth Planet. Sci. Lett.*, 1987, vol. 83, pp. 53–66.
20. Liou, J.G., Hyung Shink Kim, and Maruyama, S., Prehnite–Epidote Equilibria and Their Petrologic Applications, *J. Petrol.*, 1983, vol. 24, no. 4, pp. 321–342.
21. Liou, J.G., Maruyama, S., and Cho, M., Phase Equilibria and Mixed Parageneses of Metabasites in Low-Grade Metamorphism, *Mineral. Mag.*, 1985, vol. 352, no. 4, pp. 321–333.
22. Liou, J.G., de Capitani, C., and Frey, M., Zeolite Equilibria in the System $CaAl_2Si_2O_8$–$NaAlSi_3O_8$–SiO_2–H_2O, *New Zeal. J. Geol. Geophys.*, 1991, vol. 34, no. 3, pp. 293 – 301.
23. McCollom, T.M. and Shock, E.L., Fluid–Rock Interactions in the Lower Oceanic Crust: Thermodynamic Models of Hydrothermal Alteration, *J. Geophys. Res.*, 1998, vol. 103, no. B1, pp. 547–575.
24. Mironenko, M.V., Akinfiev, N.N., and Melikhova, T. Yu., GEOSHEQ—A Complex of Thermodynamic Modeling of Geochemical Systems, *Vestn. OGGGN RAN*, 2000, vol. 5, no. 15, pp. 96–97.
25. Miyashiro, A. and Shido, F., Differentiation of Gabbros in the Mid-Atlantic Ridge Near 24°N, *Geochem. J.*, 1980, vol. 14, no. 4, pp. 145–154.
26. Mottl, M.J., Metabasalts, Axial Hot Springs and the Structure of Hydrothermal Systems at Mid-Ocean Ridges, *Geol. Soc. Am. Bull.*, 1983, vol. 94, p. 161.
27. Sharkov, E.V., Abramov, S. S., Simonov, V.A., Krinov, D.I., Skolotnev, S.G., Bel'tenev, V.E., and Bortnikov, N.S., Hydrothermal Alteration and Sulfide Mineralization in Gabbroids of the Markov Deep (Mid-Atlantic Ridge, 6°N), *Geol. Rudn. Mestorozhd.*, 2007, vol. 49, no. 6, pp. 535–559 [*Geol. Ore Dep.* (Engl. Transl.), vol. 49, no. 6, pp. 467–486].
28. Shipboard Scientific Party, *Serpentine, Scientific Cruise Report*, Iferemer: Centre de Brest, 2007.
29. Shipboard Scientific Party, Drilling Mantle Peridotite Along the Mid-Atlantic Ridge from 14 to 16°N, *Ocean Drilling Program, Leg 209 Preliminary Report*, College Station, TX: Texas Univ., 2003.
30. Shock, E.L., Sassani, D.C., Willis, M., et al., Inorganic Species in Geologic Fluids: Correlations Among Standard Molal Thermodynamic Properties of Aqueous Ions and Hydroxide Complexes, *Geochim. Cosmochim. Acta*, 1997, vol. 61, pp. 907–950.
31. Silantyev, S.A. and Kostitsyn, Yu.A., Strontium Isotope Composition and Rubidium and Strontium Contents in the Rock-Forming Minerals of Amphibolites from the 15°20′ Fracture Zone, Atlantic, in Relation with Conditions of Oceanic Metamorphism, *Dokl. Akad. Nauk SSSR*, 1990, vol. 315, no. 3, pp. 707–711.
32. Silantyev, S.A., Metamorphism of the Modern Oceanic Basins, *Petrologiya*, 1995, vol. 3, no. 1, pp. 24–36.
33. Silantyev, S.A., Mironenko, M.V., Bazylev, B.A., and Semenov, Yu.V., Metamorphism Related to Hydrothermal Systems of Mid-Ocean Ridges: Experience of Thermodynamic Modeling, *Geokhimiya*, 1992, no. 7, pp. 1015–1034.
34. Silantyev, S.A., Mironenko, M.V., and Novoselov, A.A., Hydrothermal Systems in Peridotites of Slow-Spreading Mid-Oceanic Ridges. Modeling Phase Transitions and Material Balance: Downwelling Limb of a Hydrothermal Circulation Cell, *Petrologiya*, 2009a, vol. 17, no. 2, pp. 154–174 [*Petrology* (Engl. Transl.), vol. 17, no. 2, pp. 138–157].
35. Silantyev, S.A., Mironenko, M.V., and Novoselov, A.A., Hydrothermal Systems Hosted in Peridotites at Slow-Spreading Ridges. Modeling Phase Transformations and Material Balance: Upwelling Limb of the Hydrothermal Cell, *Petrologiya*, 2009b, vol. 17, no. 6, pp. 563–577 [*Petrology* (Engl. Transl.), vol. 17, no. 6, pp. 523–536].
36. Silantyev, S.A., Tsameryan, O.P., and Kononkova, N.N., Composition of Amphibole in the Metabasic Rocks of Ocean and Transition Zones: Indicators of Metamorphism and Fluid Regime, *Geokhimiya*, 1987, no. 9, pp. 1260–1272.
37. Silantyev, S.A., Origin Conditions of the Mid-Atlantic Ridge Plutonic Complex at 13–17°N, *Petrologiya*, 1998, vol. 6, no. 4, pp. 381–421 [*Petrology* (Engl. Transl.), vol. 6, no. 4, pp. 351–387].
38. Simonov, V.A., Silantyev, S.A., Milosnov, A.A., and Kolobov, V.Yu., First Data on Fluid Inclusions from Amphiboles and Plagioclases in the Metagabbroids of the 15°20¢ Fracture Zone, Central Atlantic, *Dokl. Akad. Nauk SSSR*, 1995, vol. 341, no. 5, pp. 676–681.
39. Stakes, D. and Vanko, D., Multistage Hydrothermal Alteration of Gabbroic Rocks from the Failed Mathematician Ridge, *Earth Planet. Sci. Lett*, 1986, vol. 79, nos. 1–2, pp. 75–92.
40. Sverjensky, D.A., Shock, E.L., and Helgeson, H.C., Prediction of Thermodynamic Properties of Aqueous Metal Complexes to 1000°C and 5 Kb, *Geochim. Cosmochim. Acta*, 1997, vol. 61, pp. 1359–1412.
41. Tivey, M.K., Generation of Seafloor Hydrothermal Vent Fluids and Associated Mineral Deposits, *Oceanography*, 2007, vol. 20, no. 1, pp. 50–65.
42. Vanko, D., High-Chlorine Amphiboles from Oceanic Rocks: Product of Highly-Saline Hydrothermal Fluids?, *Am. Mineral.*, 1986, vol. 71, p. 51–59.
43. Vikent'ev, I.V., *Usloviya formirovaniya i metamorfizm kolchedannykh rud* (Conditions of Formation and Metamorphism of Sulfide Ores), Moscow: Nauchnyi Mir, 2004.
44. Wagner, W. and Pruss, A., The IAPWS Formation 1995 for the Thermodynamic Properties of Ordinary Water Substance for General and Scientific Use, *J. Phys. Chem. Ref. Data*, 2002, vol. 31, no. 2, pp. 387–535.
45. Zolotov, M.Y. and Mironenko, M.V., Timing of Acid Weathering on Mars: A Kinetic-Thermodynamic Assessment, *J. Geophys. Res.*, 2007, vol. 112, p. E07006. doi:10.1029/2006JE002882